Design of RF Self-interference Cancellation Circuit for 100-W Full-Duplex Radio at 225–400 MHz

Mikko Heino, Matias Turunen, Miika Vuorenmaa, and Taneli Riihonen

Electrical Engineering, Tampere University, Finland
e-mail: firstname.lastname@tuni.fi

***Abstract*—The full-duplex (FD) technology enables future military radios to simultaneously transmit and receive (STAR) on the same and adjacent frequencies. This enhances spectral efficiency and makes simultaneous integrated tactical communications and electronic warfare operations possible as opposed to the current time- or frequency-division radios used in military applications. The main challenge in implementing full-duplex radios is the strong self-interference (SI) between the transmitter and the receiver requiring solutions how to cancel the coupling, which has been largely resolved at higher ultra high frequency (UHF) bands for low power transmission. This paper presents a radio-frequency SI cancellation circuit suitable especially for very high-power military applications at military-relevant lower UHF band (225–400 MHz). The circuit couples power from the transmitter and tunes the phase and amplitude of the signal to destructively combine with the received SI, and thus isolates the receiver and transmitter. The paper introduces a concept consisting of a 90° vector modulator and switchable delay lines for a low-loss and high-power-handling cancellation circuit that enables operation with very-high transmit powers of even up to 1 kW.**

I. Introduction

Full-duplex (FD) radio technology has gained significant scientific attention in communications to increase networks' spectral efficiency [1], [2]. Implementation of FD communication in the field of defense and security is relatively unexplored topic as practically all current military radios utilize conventional half-duplex communication. In addition to the enhanced spectral efficiency, FD operation enables also several novel concepts in military communications [3]–[5] such as protection by radio shielding [6], using jamming to facilitate signal intelligence [7] and concurrent tactical communication and jamming detection [8]. The concepts have also been demonstrated in laboratory conditions and outdoors with prototype hardware. The cancellation methods employed in FD technology have also potential to cancel the out-of-band interference between collocated military radios [9].

The main challenges to solve for employing FD radio technology in military systems are to move to other, especially lower, frequencies and to support significantly higher transmission powers [2], [10]. Successful cancellation of the self-interference requires methods in the electromagnetic antenna domain, the analog RF-frontend domain and in digital baseband. In the analog domain, several cancellation circuits have been presented before. However, so far they are implemented for power levels used in non-military communications, e.g., for below 40 dBm transmit power levels. The circuits are implemented with low-power-handling components, and include losses which would cause a significant thermal load with higher transmit powers. In addition, the implemented cancellers so far operate on frequencies from 1 GHz upwards [1]. Thus, solving these limitations is the major quest for the development of military full-duplex radios [10].

This research work was supported in part by the Academy of Finland, in part by the Support Foundation for National Defence, and in part by the Finnish Scientific Advisory Board for Defence (MATINE).

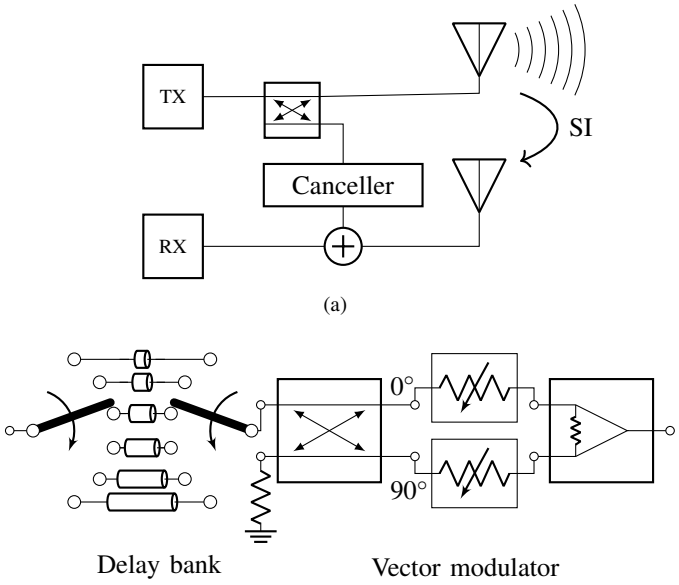

Fig. 1. Block diagram of a typical full-duplex transceiver with a canceller (a) and the designed self-interference cancellation circuit (b) that consists of a six-cable delay bank and a 90-degree vector modulator.

We develop full-duplex radio technology for the NATO harmonized UHF band I (225–400 MHz), which is considered the most appropriate frequency band to create a dedicated military band for cognitive radios due to its ideal propagation characteristics for limited range tactical radio systems [11]. As for specific modern waveforms, the band is relevant for European Secure Software Defined Radio (ESSOR) High Data Rate Waveform (HDRWF) [12], Soldier Radio Waveform [13], NATO Narrowband Waveform (NBWF) [14]–[16], and NATO Wideband Waveform (WBWF) [17]. Furthermore, we aim at

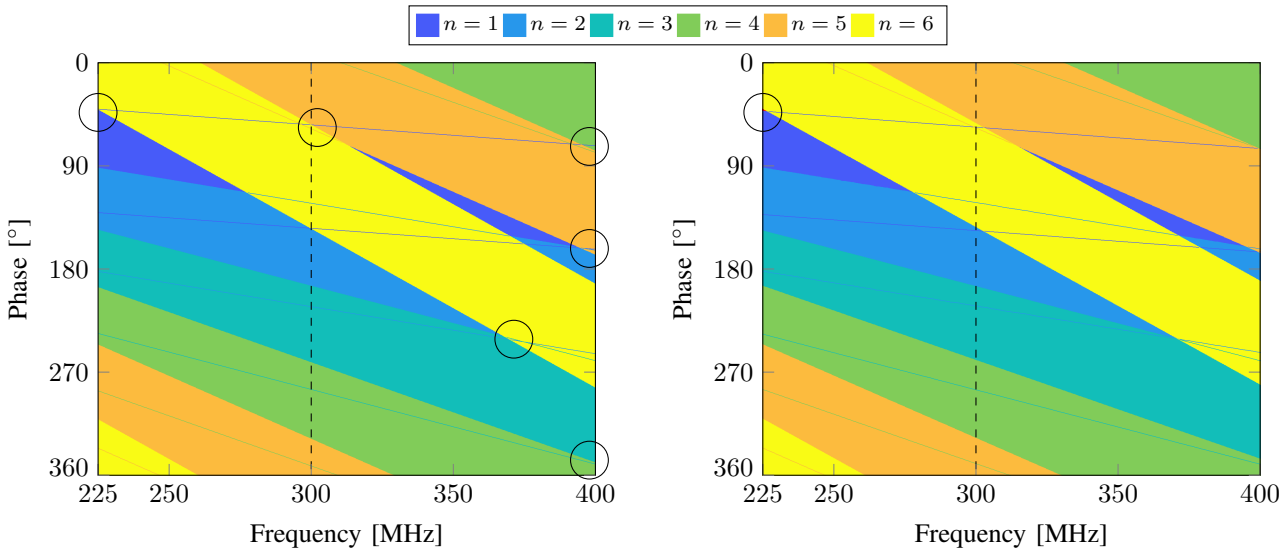

(a) Designed

(b) Measured

Fig. 2. Phase maps with 90-degree tuning range in the vector modulator. Projected and realized critical points are circled. The dashed vertical line indicates the tuning region shown in Fig. 4 at 300 MHz.

supporting at least 100-W radiated power at a transmit antenna while also maintaining scalability to kilowatt levels in some electronic warfare applications, e.g., jamming. With physical isolation between separated transmit and receive antennas or that given by a circulator in a single-antenna setup, this means that the RF cancellation circuit has to still tolerate up to several watts of input power or even tens of watts in extreme cases.

We present an original canceller design that is inspired by the wideband vector modulator usable for SI cancellation operating in the band from 1.5 to 6 GHz with insertion loss of up to 15.4 dB introduced in [18]. Our focus, however, is not in supporting wide signal bandwidths per se, but only allow tuning over the wide NATO band, which makes it feasible to reduce insertion losses by using a delay bank of six cables instead of a pair of 180-degree hybrid couplers. We demonstrate the correct operation of the design concept with simulations and measurements of a prototype.

II. High-Power Canceller Design

Analog RF cancellers operate by coupling a small amount of power from the transmitter output, tuning its amplitude and phase to be destructive to the received self-interference, and then summing it with the received signal. The basic structure of a transceiver with an RF canceller is illustrated in Fig. 1(a).

The most important part of the RF canceller is the control of the phase and amplitude of the coupled signal, i.e., 360° vector modulation. The canceller's vector modulator needs to be able to tune the phase and amplitude accurately for the whole operating frequency band to be exactly out of phase with the received self-interference and to match its amplitude. Typically, the vector modulator is implemented with an integrated circuit chip but there are no such in the market that are able to handle much power.

Here, we present a canceller structure which is made of high-power tolerant components, and at the same time is wideband to be able to operate in the band of 225–400 MHz. The canceller consists of a delay bank of six cables from which a fixed delay can be chosen with a switch. The second component is a vector modulator with amplitude control and 90° phase tuning range that is made from separate components. Together with the delay bank, the phase tuning capability is extended to 360° for the whole operating band with an amplitude tuning range of 35 to 40 dB. The system can be further adjusted for different ranges of transmitter-receiver antenna isolation by suitable selection of the TX output coupler. For example, with antenna isolation of roughly 30 dB, a 20 dB coupler could be used in the transmitter output with the rest of the amplitude tuning done in the canceller.

A. Delay Bank

The delay bank is designed so that by selecting one of the six cables together with 90° tuning range of the vector modulator, full 360° phase range is obtained for the whole frequency band. If the canceller would operate only at a point frequency, four cables would be enough as the cable delays could be chosen with 90° intervals. However, for a wide frequency band, the phase dispersion of the different delay line cables make covering each possible phase at every frequency not possible without gaps. For the considered frequency band of 225 MHz to 400 MHz, it was determined that six cables at minimum are needed to cover all possible phases. The specific cable in use can be selected by controlling two SP6T (single-pole six-throw) switches as seen in Fig. 1(b).

The chosen cable lengths are shown in Table I. Figure 2(a) shows the designed coverage area obtained with each cable from $n = 1$ to $n = 6$ in the frequency–phase domain. The

TABLE I
CABLES' SPECIFICATIONS IN THE DELAY BANK

	Designed		Measured at 225 MHz and 400 MHz		
n	l_n [mm]	delay [ns]	delay [ns]	loss [dB]	loss [dB]
1	100	0.505	0.518	0.05	0.07
2	225	1.137	1.124	0.11	0.14
3	357	1.804	1.799	0.12	0.15
4	479	2.421	2.392	0.13	0.17
5	601	3.037	3.019	0.16	0.21
6	760	3.841	3.816	0.19	0.25

thin lines show the overlapping regions between each cable. The area of a single cable consists of the phase delay due to the length of the cable and the adjustable 0 to 90° additional delay by an ideal vector modulator described by the equation

$$\phi_n = \frac{l_n f}{v_\mathrm{P}} \cdot 360^\circ + \theta, \tag{1}$$

where l_n is the length of a cable, f frequency, v_P propagation velocity in the cable, and $\theta \in [0^\circ, 90^\circ]$ the adjustable delay by the vector modulator. A standard RG-58 coaxial cable is used for the delay cable with propagation velocity $v_\mathrm{P} = 0.66\,c_0$, attenuation factor $\alpha = 0.2$ dB/m at 200 MHz, and $\alpha = 0.32$ dB/m at 400 MHz [19]. The shortest cable length in the cable bank was determined as $l_1 = 100$ mm for easy practical implementation in the prototype but it could be anything. The lengths of the other cables are determined then as additions to this length to yield the correct time delay.

It is seen in Fig. 2(a) that the phase dispersion at the highest frequency is the limiting factor in the design, i.e., the delays need to be tuned so that there is high overlap between cables at the lowest frequency so that there would not be any gaps at the highest frequency. The lengths of the cables have been tuned so that there is a minimum of 4 MHz of overlap between adjacent cables in frequency domain to increase the tolerance for manufacturing errors. The six-cable design is characterized by six critical (frequency, phase) pairs, where phase coverage gaps are most likely to occur due to imperfections:

(225 MHz, 041°), (300 MHz, 055°), (370 MHz, 240°), (394 MHz, 161°), (396 MHz, 072°), (400 MHz, 350°).

B. Vector Modulator

The detailed structure of the vector modulator is shown in Fig. 1(b). First, a 90-degree hybrid is used to divide the input power into two components, the second of which is delayed 90 degrees, i.e., to in-phase (I) and quadrature (Q) components. Then, variable attenuators are used the scale both the I- and Q-components individually. Finally, the I- and Q-components are summed again in a power combiner, thus yielding the cancellation signal which can be combined with the RX signal in the transceiver seen in Fig. 1(a). The weighting of the I- and Q-components provides a phase tuning range of maximum 0° to 90°, with the extremes achieved when either the I- or Q-component is fully suppressed.

The variable attenuators are implemented with PIN diodes as a Waugh-attenuator [20] in which the attenuation is controlled with a series bias voltage. When operated above its cut-off frequency, a PIN diode can be used as a voltage controlled variable resistor. Figure 3 shows the schematic of a single attenuator. The four diodes are obtained as an integrated SOT-25 package whereas the other components are discrete components.

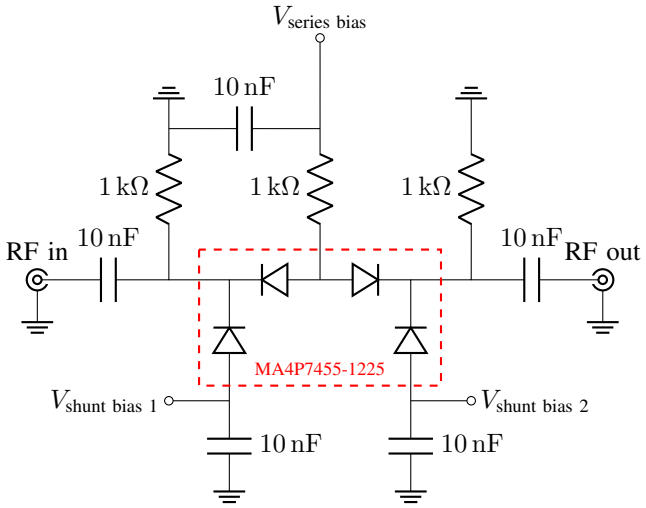

Fig. 3. Schematic of the variable attenuator in the vector modulator.

A basic configuration of a diode-based attenuator is the π-configuration, where the resistors of a fixed π-attenuator have been replaced with voltage-controlled diodes, resulting in a structure with two shunt diodes and one series diode. Proper biasing of all the diodes is used to obtain the desired attenuation and simultaneously impedance match at both the input and output. By replacing the series diode with two diodes, the biasing network can be simplified, maximum attenuation increased, and the even-order distortion products can be reduced [21]. This results in the Waugh-attenuator configuration used here.

The last element in the vector modulator is the power combiner, for which a Wilkinson power divider structure is used. The power combiner combines the I- and Q-component, with a power loss which depends on the relative amplitudes of the components.

III. Implementation and Performance Analysis

In this section, the complete canceller is first simulated with the theoretically calculated delay cable lengths in the previous section. The simulated performance is verified by measurements of a canceller prototype.

A. Simulations

For the practical implementation, first the whole canceller was simulated in Keysight ADS -software. Circuit models of the actual components were used. Mini-circuits ZX10Q-2-3-S+ was used as the 90-degree hybrid and ZMSC-2-1+ as the power combiner. The attenuator circuit shown in Fig. 3 was used for the attenuator with Macom MA4P7455-1225 diode package used for the four diodes. The diode package was selected based on its low insertion loss and high power handling.

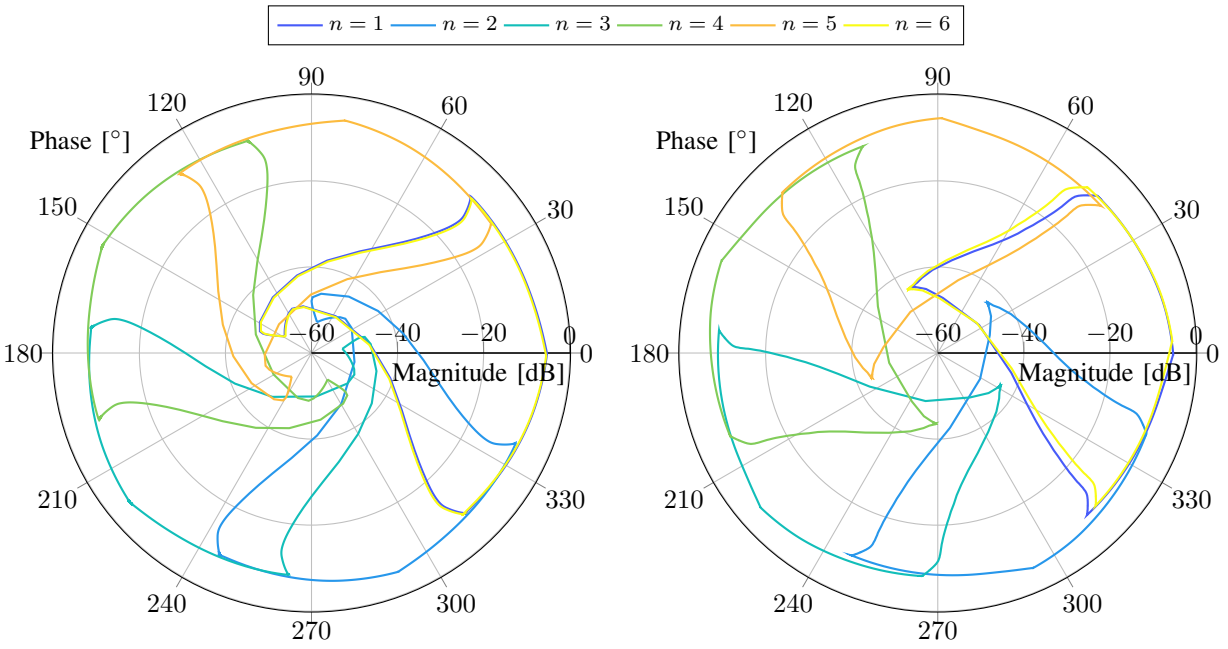

(a) Simulated (b) Measured

Fig. 4. Tuning region at 300 MHz with each cable as function of output phase and attenuation.

An RG-58 delay cable was included in the simulation and the length was changed accordingly.

Figure 4(a) shows the simulated phase and amplitude tuning range of the canceller at 300 MHz. The boundaries of the tuning range for a single cable are obtained from sweeping the first attenuator control voltage V_1 from 0 to 20 V, and keeping the second attenuator control voltage V_2 either at 0 V or 20 V, and repeated vice versa. The sweeps are repeated for each delay bank cable in Table I. A constant phase shift was added to the simulated results so that the first cable would match the phase of the measured prototype presented later. This was done to take into account the delays by the intermediate cables and PCB traces in the prototype. It is seen that full 360° range is covered with overlap between the cables, indicated also by the phase map previously. Actually, the sixth cable is redundant at 300 MHz as it covers the same phase range as the first cable as seen in Fig. 4(a). This was also predicted by the phase map in Fig. 2(a) where only five cables are needed along the dashed line at 300 MHz. However, the sixth cable is necessary for covering full phase range at other frequencies.

Figure 5 shows the simulated amplitude tuning range of the canceller for the whole frequency range when both the attenuator control voltages are equally ($V_1 = V_2$) tuned from 0 V to 20 V. It is seen that roughly 50 down to 40 dB tuning range is achieved depending on the frequency.

The phase range with a single cable moves towards higher phases when tuned to lower amplitudes, seen as counterclockwise rotation of the curves in Fig. 4(a). This is caused by the phase shift of single attenuators when controlled with low voltages seen in Fig. 7. However, this phase rotation occurs with each cable and thus full 360° coverage is still obtained.

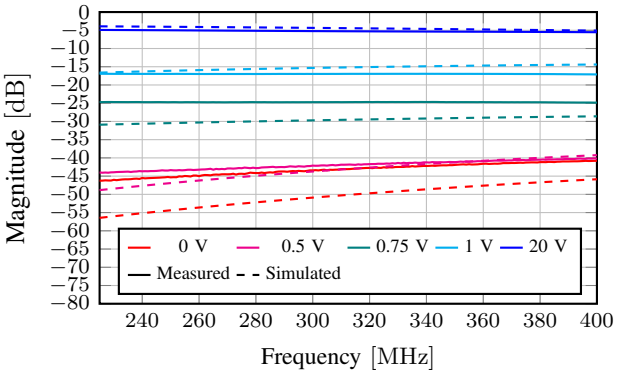

Fig. 5. Amplitude tuning range of the vector modulator when both attenuators are tuned with equal voltages ($V_1 = V_2$).

B. Measurements

First, the cables were manufactured based on the lengths designed for the phase map. Table I shows the delays of the simulated and measured cables, and the losses of the measured cables at both ends of the frequency range. It is seen that the desired delays were reached within 3 % accuracy. Fig. 2(b) shows the phasemap obtained from the measured cables. When comparing to the simulated phase map, it is seen that most of the critical points were covered even though there are slight errors in the cable lengths. However, there is a very small hole formed at (225 MHz, 41°) in the measured phasemap. The gap in missing phase values is only 2° wide, therefore the effect to real-world performance is minimal.

A prototype of the vector modulator was manufactured

based on the simulations. The two attenuators based on Fig. 3 were implemented on two small PCBs. Discrete components with connectors were used for the 90-degree hybrid and the power combiner, which were connected to the attenuators with coaxial cables. The delay bank cables were connected one-by-one to the hybrid, i.e., SP6T switches were not yet used for the measurement in this initial study. Figure 6 shows the manufactured vector modulator with external DC cables providing the bias voltages to control the attenuators.

The performance of the prototype — the vector modulator together with the delay cables — was measured with a vector network analyzer (VNA). Figure 5 shows the measured attenuation range of the vector modulator while Fig. 4(b) shows the measured phase-magnitude tuning region at 300 MHz. It is seen that for high control voltages the attenuation follows closely the simulations. However, for voltages below 1 V, the attenuation deviates from the simulated value, and the maximum attenuation is 5 to 10 dB lower for the measured prototype, i.e., the measured attenuators do not have as high isolation as the simulated ones. The difference in the measured and simulated plots at low magnitudes can be seen also in Fig. 7 at control voltages below 2 V.

The prototype has some non-idealities. The 90-degree hybrid has a phase unbalance of 3° to 4°, and amplitude unbalance of 0.7 dB at the operating band. The attenuators have non-linear phase and magnitude response when tuning the control voltage. The power combiner has a maximum phase and amplitude unbalance of 4° and 0.3 dB. The components have limited isolation and slight mismatch which can cause slight errors due to reflections. The non-idealities cause deviation from the designed performance, however, the overlap between cables still enables successful operation. If needed, the nonlinear part of the attenuator phase response in Fig. 7 can be avoided by selecting the TX output coupler such that canceller attenuator remains in the linear phase range.

The longest cable at the top frequency has 0.25 dB loss, the 90-degree hybrid a typical insertion loss of 0.6 dB, a single attenuator an adjustable insertion loss from 1.4 dB to 37 dB, the power combiner 0.6 dB with additional loss of 3 dB when the I- and Q-components are equal. This renders worst-case insertion loss of 6 dB. When the TX power is 100 W and a 10 dB coupler is used for canceller input, in the worst case, 0.6 W is lost in the cable, 1.2 W in the hybrid, 2.4 W at minimum in the attenuators, and 3.3 W in the power combiner. This corresponds to situation of roughly 16 dB antenna isolation.

The maximum input powers of the hybrid and the attenuator are 15 W and 20 W, respectively, so they fulfill the power requirement easily. However, the internal dissipation limit of the combiner used in the preliminary prototype is only 0.125 W. The future next prototype version will employ a high-power combiner, e.g., Mini-Circuits SYPS-2-52HP+, with dissipation limit of 6 W — this enables even higher powers than 100 W to be used. Furthermore, the power handling requirement depends heavily on antenna isolation, which is usually higher than 16 dB required with the above numbers. Increasing the antenna isolation would enable even higher TX powers to be used.

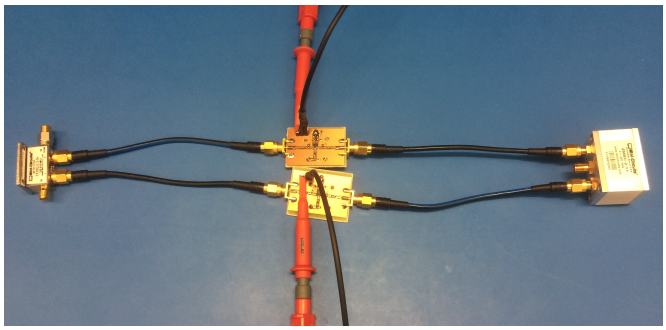

Fig. 6. Prototype of the vector modulator part of the canceller.

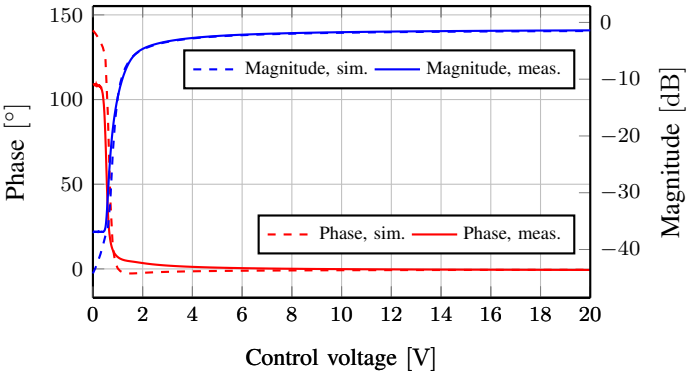

Fig. 7. Phase non-linearity of a single attenuator when tuning the control voltage.

IV. Conclusion

In this paper, we presented the design of an analog self-interference cancellation circuit for the military-relevant 225–400 MHz band and beyond 100-W power handling. The design comprises a wideband 90-degree vector modulator, which is implemented with PIN-diode-based variable attenuators, and a bank of six delay lines for achieving full 360° tuning range for all frequencies in the band. The viability of the concept was demonstrated with simulations and measuring the delay bank's cables and a vector modulator prototype. The next research steps will be to implement a full, revised prototype of the cancellation circuit and demonstrate the actual cancellation performance as well as to design and implement control electronics and algorithms along the lines of [22]–[24]. We also consider using multiple parallel cancellers with different delay lines for multipath cancellation.

References

[1] K. E. Kolodziej, B. T. Perry, and J. S. Herd, "In-band full-duplex technology: Techniques and systems survey," *IEEE Transactions on Microwave Theory and Techniques*, vol. 67, no. 7, pp. 3025–3041, July 2019.

[2] Task Group IST-ET-101, "Full-duplex radio — Increasing the spectral efficiency for military applications," NATO Science and Technology Organization, Tech. Rep., Jan. 2020.

[3] K. Pärlin and T. Riihonen, *Full-duplex transceivers for defense and security applications*. Springer Singapore, 2020, pp. 249–274.

[4] M. Adrat, R. Keller, M. Tschauner, S. Wilden, V. Le Nir, T. Riihonen, M. Bowyer, and K. Pärlin, "Full-duplex radio — Increasing the spectral efficiency for military applications," in *Proc. International Conference on Military Communications and Information Systems*, May 2019.

[5] T. Riihonen, D. Korpi, O. Rantula, H. Rantanen, T. Saarelainen, and M. Valkama, "Inband full-duplex radio transceivers: A paradigm shift in tactical communications and electronic warfare?" *IEEE Communications Magazine*, vol. 55, no. 10, pp. 30–36, Oct. 2017.

[6] T. Riihonen, D. Korpi, M. Turunen, T. Peltola, J. Saikanmäki, M. Valkama, and R. Wichman, "Military full-duplex radio shield for protection against adversary receivers," in *Proc. International Conference on Military Communications and Information Systems*, May 2019.

[7] T. Riihonen, D. Korpi, M. Turunen, T. Peltola, J. Saikanmäki, M. Valkama, and R. Wichman, "Tactical communication link under joint jamming and interception by same-frequency simultaneous transmit and receive radio," in *Proc. IEEE Military Communications Conference*, Oct. 2018.

[8] T. Riihonen, M. Turunen, K. Pärlin, M. Heino, J. Marin, and D. Korpi, "Full-duplex operation for electronic protection by detecting communication jamming at transmitter," in *Proc. IEEE International Symposium on Personal, Indoor and Mobile Radio Communications*, Sept. 2020.

[9] T. Ranström and E. Axell, "Full duplex based digital out-of-band interference cancellation for collocated radios," in *Proc. Wireless Communications and Networking Conference*, May 2020.

[10] T. Riihonen, "Military applications," in *In-Band Full-Duplex Wireless Systems Handbook*, K. E. Kolodziej, Ed. Artech House, Mar. 2021, ch. 17.

[11] B. Scheers, "Introduction of dynamic spectrum access technology in NATO Europe tactical communications," in *Proc. IEEE Military Communications Conference*, Nov. 2013.

[12] C. Serra, P. Margot, P. Heikkinen, A. Quintana, M. Lewandowski, B. Granbom, C. Armani, and Y. Thomas, "ESSOR HDRWF — Capabilities and perspectives of an innovative coalition waveform," in *Proc. IEEE Military Communications Conference*, Nov. 2013.

[13] M. S. Marwick, C. M. Kramer, and E. J. Laprade, "Analysis of Soldier Radio Waveform performance in operational test," Institute for Defense Analyses, Tech. Rep., May 2015.

[14] E. Casini, D. Fertonani, and G. Colavolpe, "Advanced CPM receiver for the NATO tactical Narrowband Waveform," in *Proc. IEEE Military Communications Conference*, Oct.–Nov. 2010.

[15] L. Li, H. Rutagemwa, J. Hu, P. Hugg, P. Vigneron, C. Brown, and T. Kunz, "Networking for next generation NBWF radios," in *Proc. IEEE Military Communications Conference*, Oct. 2015.

[16] V. Le Nir and B. Scheers, "Low complexity generic receiver for the NATO Narrow Band Waveform," in *Proc. International Conference on Military Communications and Information Systems*, May 2017.

[17] R. Matyszkiel, R. Polak, P. Kaniewski, and D. Laskowski, "The results of transmission tests of Polish broadband SDR radios," in *Proc. Communication and Information Technologies*, Oct. 2017.

[18] K. E. Kolodziej and B. T. Perry, "Wideband vector modulator for RF cancellers in STAR systems," in *Proc. IEEE Radio and Wireless Symposium*, Jan. 2018.

[19] Huber+Suhner, "Huber+suhner flexible RF cable RG_58_CU datasheet," Tech. Rep., Jan. 2021. [Online]. Available: https://ecatalog.hubersuhner.com/media/documents/datasheet/en/pdf/22510015

[20] R. W. Waugh, "A low cost surface mount PIN diode π attenuator," *Microwave Journal*, vol. 35, no. 5, pp. 280–284, May 1992.

[21] Hewlett-Packard, "Application note 1048: A low-cost surface mount PIN diode π attenuator," Tech. Rep. [Online]. Available: http://www.hp.woodshot.com/hprfhelp/4_downld/lit/diodelit/an1048.pdf

[22] K. E. Kolodziej, A. U. Cookson, and B. T. Perry, "In-band full-duplex RF canceller tuning using adaptive learning rate functions," in *Proc. IEEE Radio and Wireless Symposium*, Jan. 2020.

[23] K. E. Kolodziej, A. U. Cookson, and B. T. Perry, "Machine learning for accelerated IBFD tuning in 5G flexible duplex networks," in *Proc. IEEE MTT-S International Microwave Symposium*, Aug. 2020.

[24] K. E. Kolodziej, A. U. Cookson, and B. T. Perry, "Adaptive learning rate tuning algorithm for RF self-interference cancellation," *IEEE Transactions on Microwave Theory and Techniques*, vol. 69, no. 3, Mar. 2021.